

Density-Adaptive Kernel based Re-Ranking for Person Re-Identification

Ruo-Pei Guo, Chun-Guang Li, Yonghua Li and Jiaru Lin

School of Information and Communication Engineering

Beijing University of Posts and Telecommunications, Beijing 100876, P.R. China

{guo2016; lichunguang; liyonghua; jrlin}@bupt.edu.cn

Abstract—Person Re-Identification (ReID) refers to the task of verifying the identity of a pedestrian observed from non-overlapping surveillance cameras views. Recently, it has been validated that re-ranking could bring extra performance improvements in person ReID. However, the current re-ranking approaches either require feedbacks from users or suffer from burdensome computation cost. In this paper, we propose to exploit a density-adaptive kernel technique to perform efficient and effective re-ranking for person ReID. Specifically, we present two simple yet effective re-ranking methods, termed inverse Density-Adaptive Kernel based Re-ranking (inv-DAKR) and bidirectional Density-Adaptive Kernel based Re-ranking (bi-DAKR), which are based on a smooth kernel function with a density-adaptive parameter. Experiments on six benchmark data sets confirm that our proposals are effective and efficient.

I. INTRODUCTION

Person Re-Identification (ReID) refers to the task of verifying the identity of a pedestrian observed from non-overlapping surveillance cameras views [1]. Due to its importance for the public security, it has received a lot of attention and increasingly becomes one of the most critical tasks in video analysis. However, the task of ReID is quite challenging, because the views captured by the surveillance cameras are under unconstrained conditions, and thus the obtained images contain large variations from the changes of pose, viewpoint, and illumination, occlusion, blur, background, etc.

To tackle these challenges, the standard pipeline of a person ReID system usually consists of two components: a) feature extraction, and b) metric learning. In the existing works, majority of efforts have been cast into extracting robust and discriminative visual representation. It has been verified that the local features, *i.e.*, color or oriented gradient histogram [2], [3], [4], [5], [6] are effective for person ReID, and combining multiple types of features, *i.e.*, color, texture, and spatial structure, is useful to find more informative matchings [7], [8], [9], [10], [11], [12], [13], [14]. On the other hand, metric learning methods—which learn a discriminative distance metric or equivalently a low-dimensional subspace have found that a new feature space, where the samples of same person are closer, could help the task of finding informative matchings [15], [16], [17], [18], [19], [20], [21].

A. Related Work

In this paper, we concern the task of finding the best matches when a gallery set is available. In image retrieval, this is a re-

ranking problem. Recently, it has been reported that re-ranking could bring extra performance improvement for a person ReID system [22], [23], [24], [25], [26]. For example, feedback knowledge from users could be used to refine the ranking results, *i.e.*, [22], [23]. However, the feedback based refinement approaches build upon persistent feedbacks from users, which is an expensive burden on users. In [25], an approach called Supervised Smoothed Manifold (SSM) is proposed, in which an affinity graph is built to capture the manifold structure in the gallery set and the pairwise supervision information is propagated on the affinity graph. However, building the affinity graph is computationally expensive because all the samples in the gallery set will be involved. As an alternative way, context information among a given query and its k nearest neighbors are exploited to refine the ranking result. The typical approaches are mainly based on the k -reciprocal nearest neighbors, as illustrated in Fig.1(c), that is, the matched two people usually take each other as one of its neighbors [24], [27], [28], [29], [30], [31]. In [27], [28], [30], the k -reciprocal nearest neighbors are directly considered as the top-ranked results. Recently, in [24], [29], the k -reciprocal nearest neighbors are encoded to refine the initial ranking list, or even integrated with local query expansion and Jaccard distance. In [31], extra visual features are combined with the k -reciprocal nearest neighbors to optimize the ranking list. However, these methods either suffer from the sensitivity to the parameters or heavy computation burden.

B. Contributions

Different from the prior work mentioned above, we attempt to exploit a *density-adaptive kernel technique* to perform efficient and effective re-ranking for person ReID. Specifically, we propose two Density-Adaptive Kernel based Re-ranking (DAKR) methods, called inverse DAKR (inv-DAKR) and bidirectional DAKR (bi-DAKR), in which inv-DAKR is a “soft” version of the k -inverse nearest neighbors method [32] and bi-DAKR is a “soft” version of the k -reciprocal nearest neighbors method, respectively. In both inv-DAKR and bi-DAKR, the local density information of each sample in gallery set is used to define an adaptive local parameter in the kernel function. By doing so, unlike in k -inverse nearest neighbors and k -reciprocal nearest neighbors, inv-DAKR and bi-DAKR can accommodate the ambiguity and local density information

arXiv:1805.07698v1 [cs.CV] 20 May 2018

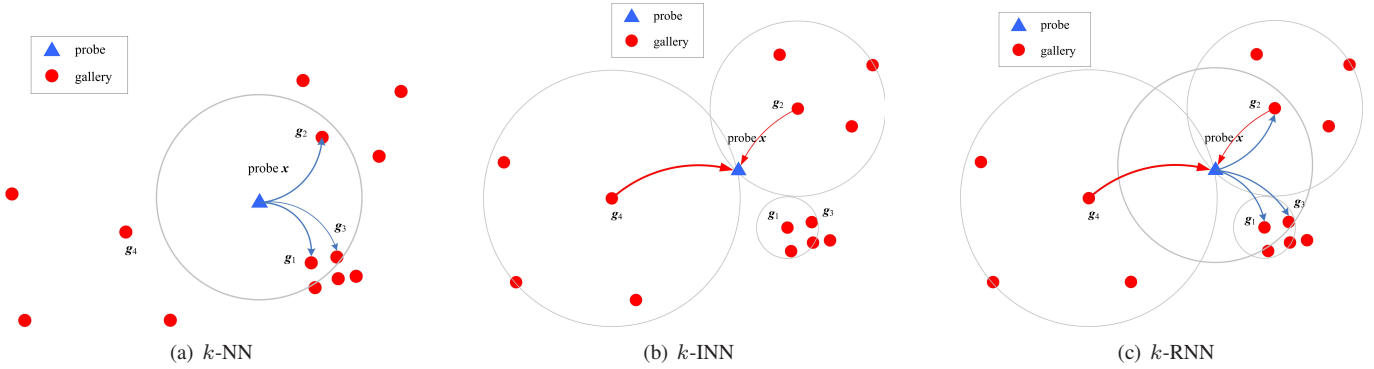


Fig. 1. Illustration for ranking and re-ranking in person ReID. (a) k -NN; (b) k -INN for inverse re-identification; (c) k -RNN, *i.e.*, k -NN integrated with k -INN, for bidirectional re-identification. The big circles indicate the boundary of the local neighborhood specified by 3-nearest neighbors.

in the ranking results. By exploiting the symmetry in formulation, the computational burden is reduced. Experiments on benchmark data sets confirm that our proposals are effective and efficient.

II. PROBLEM FORMULATIONS AND STATEMENTS

To introduce our proposals, we review the prior methods for ranking or re-ranking by grouping them into three categories: a) k -nearest neighbors (k -NN) based methods, b) k -inverse nearest neighbors (k -INN) based methods, and c) k -reciprocal nearest neighbors (k -RNN) based methods. Suppose that a gallery set $X = \{\mathbf{x}_1, \dots, \mathbf{x}_N\}$ is given, where $\mathbf{x}_j \in \mathbb{R}^d$.

A. k -Nearest Neighbors based Methods

One calculates the distance between the probe \mathbf{x}_0 and each sample \mathbf{x}_j in the gallery set X , and finds a set of best matching candidates from the gallery set X . Precisely, finding the top- k candidates can be formulated as follows:

$$\mathcal{N}(\mathbf{x}_0, k) = \arg \min_{\mathbf{x}_j \in X}^{[1:k]} \|\mathbf{x}_j - \mathbf{x}_0\|, \quad (1)$$

where $\|\cdot\|$ is a distance metric predefined or learnt from data, $\mathcal{N}(\mathbf{x}_0, k)$ is the set of the k -NNs of the probe \mathbf{x}_0 , and $[1:k]$ indicates to take the first k results from a sorted list. The true match is expected to be included in $\mathcal{N}(\mathbf{x}_0, k)$. In Fig.1(a), the blue links starting from the probe \mathbf{x}_0 to the samples $\{\mathbf{g}_1, \mathbf{g}_2, \mathbf{g}_3\}$ in the gallery set illustrate result of k -NN. In this case, \mathbf{g}_1 is the best matching sample to the probe \mathbf{x}_0 (because \mathbf{g}_1 is slightly nearby to \mathbf{x}_0 than \mathbf{g}_2).

While it is simple and efficient in implementation, it exploits only the information in a local neighborhood of the probe, without leveraging more information of the local neighborhood of samples in gallery set.

B. k -Inverse Nearest Neighbors based Methods

To exploit more information in the gallery set, it is interesting to use k -INN, which is developed in [32]. Specifically, in k -INN, for each sample \mathbf{x}_j in the gallery set X , we find the best matching to \mathbf{x}_j from $\{\mathbf{x}_0\} \cup X_{-j}$, *i.e.*,

$$\mathcal{N}(\mathbf{x}_j, k) = \arg \min_{\mathbf{x}_i \in \{\mathbf{x}_0\} \cup X_{-j}}^{[1:k]} \|\mathbf{x}_i - \mathbf{x}_j\|, \quad (2)$$

where X_{-j} is the gallery set without the j -th sample \mathbf{x}_j . Then, \mathbf{x}_j is viewed as one of the k -INNs of \mathbf{x}_0 if the probe \mathbf{x}_0 is included in $\mathcal{N}(\mathbf{x}_j, k)$. To find out all the k -INNs of \mathbf{x}_0 , one has to compute $\mathcal{N}(\mathbf{x}_j, k)$ for all $j = 1, \dots, N$. Denote $\mathcal{I}(\mathbf{x}_0, k)$ as the set of all k -INNs of \mathbf{x}_0 . If $\mathbf{x}_j \in \mathcal{I}(\mathbf{x}_0, k)$, the probe \mathbf{x}_0 is accepted as a good match of \mathbf{x}_j ; otherwise, \mathbf{x}_0 is rejected by \mathbf{x}_j . The true match is expected to be included in $\mathcal{I}(\mathbf{x}_0, k)$. In Fig.1(b), the red links starting from the gallery samples $\{\mathbf{g}_2, \mathbf{g}_4\}$ to the probe \mathbf{x}_0 illustrate the k -INNs where $k = 3$.

In previous work [24], [27], [28], [29], [30], k -INN is considered as an intermediate step. However, when N is large, finding $\mathcal{I}(\mathbf{x}_0, k)$ is quite time consuming. Moreover, the ambiguity of the potential matching candidates is ignored in the returned results. In experiments, we list it as a re-ranking method and present extensive evaluations.

C. k -Reciprocal Nearest Neighbors based Methods

Recall that, in logic, an identification (\Leftrightarrow) consists of implications from two directions (\Rightarrow and \Leftarrow). Therefore, it is natural to integrate the k -NN and the k -INN to form a *bidirectional identification*, as illustrated in Fig.1(c), which is a concept called k -RNN. Denote the k -RNNs of \mathbf{x}_0 as $\mathcal{R}(\mathbf{x}_0, k)$. Then, $\mathcal{R}(\mathbf{x}_0, k)$ is the intersection of $\mathcal{N}(\mathbf{x}_0, k)$ and $\mathcal{I}(\mathbf{x}_0, k)$, *i.e.*, $\mathcal{R}(\mathbf{x}_0, k) = \mathcal{N}(\mathbf{x}_0, k) \cap \mathcal{I}(\mathbf{x}_0, k)$. The k -RNN is illustrated in Fig.1(c). In this case, by integrating k -NN and k -INN, \mathbf{g}_2 will be the candidate match to the probe \mathbf{x}_0 when $k = 3$.

While it has been verified that the performance of ReID could be improved, the previous work, *e.g.*, [27], [28], [29], [30], [24], still suffer from two limitations: a) The ambiguity and density information of the potential matching candidates is ignored in the returned k -INNs and thus in the k -RNNs; b) Due to ignorance of the ambiguity, the performance of k -RNN based methods are sensitive to parameter k .

III. OUR PROPOSAL: DENSITY-ADAPTIVE KERNEL BASED RE-RANKING

To tackle the limitations aforementioned, we propose to exploit a *density-adaptive kernel technique* to carry out the insight of k -RNN to perform efficient and effective re-ranking for person ReID. To be more specific, rather than finding k -NN which has a hard boundary, we put a smooth kernel function with an adaptive local parameter at each sample, and use

the responses of the kernel function to define re-identification scores of continuous value. The scores of continuous value can accommodate the ambiguity in ranking or re-ranking list whereas the adaptive local parameter encodes the local density information into the ranking or re-ranking.

A. Density-Adaptive Kernel Function

To accommodate the ambiguity in ranking, we use a smooth kernel function to compute the neighboring information in k -NNs, rather than just keeping k -NNs. Specifically, given a probe \mathbf{x}_0 , we put a *radial basis function* $\kappa(\mathbf{x}|\mathbf{x}_0, \sigma_0)$ at point \mathbf{x}_0 , i.e.,

$$\kappa(\mathbf{x}|\mathbf{x}_0, \sigma_0) = \phi\left(\frac{\|\mathbf{x} - \mathbf{x}_0\|_2}{\sigma_0}\right), \quad (3)$$

where σ_0 is a local parameter. To encode the local density information, as in [33], we define σ_0 via the distance of \mathbf{x}_0 to its k -th nearest neighbor $\mathbf{x}_0^{(k)}$ in the gallery set X , i.e., $\sigma_0 = \|\mathbf{x}_0 - \mathbf{x}_0^{(k)}\|_2$, where $k \geq 1$ is a preset parameter.

The advantages of using a smooth kernel function with a density-adaptive parameter will be exploited in finding k -INNs or k -RNN, which will be presented in the next.

B. Inverse Density-Adaptive Kernel Re-Ranking (inv-DAKR)

The key ingredient of inv-DAKR lies that, instead of finding k -INN directly, we use a smooth kernel function with an adaptive parameter to select k -INNs.

Specifically, we put a *radial basis function* $\kappa(\mathbf{x}|\mathbf{x}_j, \sigma_j)$ at each data point \mathbf{x}_j in the gallery set, i.e.,

$$\kappa(\mathbf{x}|\mathbf{x}_j, \sigma_j) = \phi\left(\frac{\|\mathbf{x} - \mathbf{x}_j\|_2}{\sigma_j}\right), \quad (4)$$

where σ_j is an adaptive local parameter and $j = 1, \dots, N$.

The expected σ_j should be density-adaptive. In a denser region, the parameter σ_j should be smaller in order to make the scoring function be more selective (or sensitive) to reject more samples; whereas in a sparser region, the parameter σ_j should be larger in order to make the scoring function be relatively inclusive (or less sensitive) to accept more samples. To encode the density information in the local neighborhood of \mathbf{x}_j , again, we define σ_j as the distance of \mathbf{x}_j to its k -th nearest neighbor $\mathbf{x}_j^{(k)}$ in X_{-j} , i.e., $\sigma_j = \|\mathbf{x}_j - \mathbf{x}_j^{(k)}\|_2$, where $k \geq 1$ is a preset parameter.

C. Bidirectional Density-Adaptive Kernel Re-Ranking (bi-DAKR)

To implement bi-DAKR, we gather scores from the direct way (i.e. k -NN) and the inverse way (i.e. k -INN). Interestingly, the deployed density-adaptive kernel functions in (3) and (4) are well-prepared to define a bidirectional re-identification.

To be more specific, for a sample \mathbf{x}_j in the gallery set:

- In the direct way, the scoring of \mathbf{x}_j from the probe \mathbf{x}_0 will be $\kappa(\mathbf{x}_j|\mathbf{x}_0, \sigma_0) = \phi\left(\frac{\|\mathbf{x}_j - \mathbf{x}_0\|_2}{\sigma_0}\right)$;
- In the inverse way, the scoring of the probe \mathbf{x}_0 from \mathbf{x}_j will be $\kappa(\mathbf{x}_0|\mathbf{x}_j, \sigma_j) = \phi\left(\frac{\|\mathbf{x}_0 - \mathbf{x}_j\|_2}{\sigma_j}\right)$.

TABLE I
COMPUTATION COMPLEXITY COMPARISON.

Methods	Complexity	
k -NN	$O(N + N \log_2 N)$	
k -INN	$O(N(N+1)[1 + \log_2(N+1)] + N \log_2 N)$	
k -RNN	$O(N(N+1)[1 + \log_2(N+1)] + N(1 + \log_2 N))$	
inv-DAKR	off-line	$O(N^2 + N^2 \log_2 N)$
bi-DAKR	on-line	$O(N + N \log_2 N)$ $O([2N + 2N \log_2 N])$

The reasons to use the radial basis function are twofold: a) the function $\phi\left(\frac{\|\cdot\|_2}{\sigma}\right)$ has an explicit connection to the distance function, and b) the radical symmetry in kernel function $\phi\left(\frac{\|\cdot\|_2}{\sigma}\right)$ makes the two directions share the same calculation because $\|\mathbf{x}_j - \mathbf{x}_0\|_2 = \|\mathbf{x}_0 - \mathbf{x}_j\|_2$.

In this paper, we investigate the following three simple rules to define the bidirectional scorings.

- Rule 1 (additive):

$$\chi_1(\mathbf{x}_0, \mathbf{x}_j) = \phi\left(\frac{\|\mathbf{x}_j - \mathbf{x}_0\|_2}{\sigma_0}\right) + \phi\left(\frac{\|\mathbf{x}_0 - \mathbf{x}_j\|_2}{\sigma_j}\right). \quad (5)$$

- Rule 2 (multiplicative):

$$\chi_2(\mathbf{x}_0, \mathbf{x}_j) = \phi\left(\frac{\|\mathbf{x}_j - \mathbf{x}_0\|_2}{\sigma_0}\right) \cdot \phi\left(\frac{\|\mathbf{x}_0 - \mathbf{x}_j\|_2}{\sigma_j}\right). \quad (6)$$

- Rule 3 (melt-out multiplicative):

$$\chi_3(\mathbf{x}_0, \mathbf{x}_j) = \phi\left(\frac{\|\mathbf{x}_j - \mathbf{x}_0\|_2 \cdot \|\mathbf{x}_0 - \mathbf{x}_j\|_2}{\sigma_0 \sigma_j}\right). \quad (7)$$

Remark 1. The efficiency of inv-DAKR and bi-DAKR for re-ranking comes from the facts that the symmetry in formulation with the help of a density-adaptive parameter σ_j (which could be pre-computed in advance) reduces the inverse identification into the same form as the direct identification. Note that, only a density-adaptive parameter σ_0 needs to be computed at the testing phase in bi-DAKR. For clarity, we list the computation complexity of inv-DAKR and bi-DAKR compared to the baselines (k -NN, k -INN and k -RNN) in Table I.

Remark 2. Compared to the previous work [24], [27], [28], [30], [29], the effectiveness of inv-DAKR and bi-DAKR comes from two aspects. On one hand, the smoothness of kernel functions used in inv-DAKR and bi-DAKR are able to model the ambiguity in the potential candidates, rather than using a binary decision to judge in or not in the list of k -nearest neighbors. Especially, the used local parameter encodes the density information in each local neighborhood and thus makes inv-DAKR and bi-DAKR more accurate. On the other hand, in inv-DAKR and bi-DAKR, all samples in the gallery set are used to find the k -RNNs of the probe, rather than using a small subset of the samples in gallery set, i.e., the k -nearest neighbors of the probe. Especially, if the true matching is not in the k -NNs of the probe \mathbf{x}_0 , then finding k -INNs and k -RNNs from the k -NNs of the probe \mathbf{x}_0 will be blind.

IV. EXPERIMENTAL EVALUATIONS

To validate the efficiency and effectiveness of our proposals, we conduct experiments on six benchmark data sets, including GRID [34], PRID450S [35], VIPeR [10], CUHK03 [36], Market-1501 [37] and Mars [38].

TABLE II
COMPARISON ON GRID WITH DIFFERENT FEATURES.

Feature	Methods	r=1	r=10	r=20
ELF6	k -NN	8.64	30.48	44.32
	k -INN	13.60	38.96	50.88
	k -RNN	10.96	37.44	48.72
	inv-DAKR	13.36	40.16	52.08
	bi-DAKR	11.28	39.52	52.40
	bi-DAKR [†]	11.28	39.44	52.32
	bi-DAKR [‡]	11.44	39.44	52.32
FusionAll	k -NN	27.20	61.12	71.20
	k -INN	28.56	59.92	70.00
	k -RNN	26.08	57.84	69.20
	inv-DAKR	28.88	60.40	70.88
	bi-DAKR	28.08	62.40	72.08
	bi-DAKR [†]	28.08	62.40	72.08
	bi-DAKR [‡]	28.08	62.32	72.08
	re-ranking[24]	28.24	61.60	71.92
	SSM[25]	27.60	62.56	71.60

A. Experiment Protocol

We use the standard protocol to split data in our experiments. The matching accuracy at different ranks on data sets GRID, PRID450S, VIPeR, and CUHK03 is averaged over 10 trials. For bi-DAKR, we denote Rule 3 in (7) as bi-DAKR, and denote Rule 1 in (5) and Rule 2 (6) as bi-DAKR[†] and bi-DAKR[‡], respectively. As baselines, we consider k -NN, k -INN, k -RNN, SSM [25], and re-ranking [24].

Note that re-ranking can be viewed as a postprocessing step for person ReID. Our proposed inv-DAKR and bi-DAKR can be inserted into any person ReID pipeline. Therefore, we evaluate inv-DAKR and bi-DAKR on the six data sets with different combinations of feature extraction and metric learning. For GRID, PRID450S, VIPeR, and CUHK03, we use LOMO [13] and GOG [12] features; whereas for Market-1501 and Mars, we use IDE features [37], [38]. For GRID, we also use ELF6 features [4]. Moreover, we conduct experiments on concatenating LOMO with GOG features and named it as *Fusion*. In addition, another fusion feature is introduced for GRID by equally concatenating *Fusion* with unit ℓ_2 normalized ELF6 features and marked it as *FusionAll*. On the other hand, for metric learning, we also consider Euclidean distance (ℓ_2 norm), Mahalanobis distance, and KISSME [17] in both Market-1501 and Mars. Note that in inv-DAKR and bi-DAKR, the density-adaptive parameter σ_j depends on a preset value k , which changes from dataset to dataset. For each dataset, we report the results with an optimal k .

B. Evaluation on GRID, PRID450s, VIPeR, and CUHK03

We conduct extensive experiments on data sets GRID, PRID450s, VIPeR, and CUHK03 with LOMO, GOG, and a fusion of LOMO and GOG, in which metric learning method XQDA [13] is adopted. Experimental results are presented in Tables II and III. It could be observed that:

- Compared to the baselines, the proposed inv-DAKR and bi-DAKR show notable performance improvements. These results confirm the effectiveness of inv-DAKR and bi-DAKR.
- For the three rules to form bi-DAKR, including bi-DAKR, bi-DAKR[†], and bi-DAKR[‡], there is no significant

difference. Thus, we report evaluations only with bi-DAKR thereafter.

- Compared to inv-DAKR, the performance of bi-DAKR is more promising. This suggests that integrating the direct way and the inverse way of re-identifications is useful.
- The k -INN and k -RNN based methods show better performance on small data set GRID, compared to k -NN. However, when data set becomes large, lacking ambiguity and efficiency are the major bottlenecks in them. Thus, we report the results of k -NN hereafter.

C. Evaluation on Market-1501 and Mars

Experimental results on Market-1501 and Mars are shown in Tables IV, and V. Again, we can observe the performance improvements over the baseline method k -NN and bi-DAKR performs slightly better than inv-DAKR. Compared to the re-ranking method proposed in [24], the accuracy of inv-DAKR and bi-DAKR is inferior on rank-1 and mAP. However, the best performance of the re-ranking method in [24] on rank-5, rank-10 and rank-20 is not as good as inv-DAKR and bi-DAKR. In [24], local query expansion and Jaccard metric are used to refine the ranking list. However, when the size of the neighborhood grows, it is hard for the local query expansion and Jaccard metric to find good matchings. Besides, it should be mentioned that the re-ranking method in [24] is very sensitive to parameters (*i.e.*, k_1 , k_2 , λ); whereas inv-DAKR and bi-DAKR are not sensitive to the single parameter k , which will be shown in subsection IV-E.

D. Comparison on Time Costs

For fair comparison, we list the computational time costs in Table VI. For data set CHUK03, we report time cost of the labeled data set. The size in table is of data set for test. It shows that in both situations, the time costs of our proposals are much lower than the re-ranking method [24], especially when the dataset is large. In [24], it needs to find k -reciprocal nearest neighbors, expand local query sequence, and compute Jaccard distance; whereas in our inv-DAKR and bi-DAKR, only an adaptive kernel function is evaluated. Though slightly defeated by the re-ranking method in [24] at rank-1 and mAP, our inv-DAKR and bi-DAKR are much simpler, faster, and having improved results at rank-5, rank-10 and rank-20.

E. Evaluation on Parameter k Used to Set σ_j

Note that parameter σ_j is set as the distance of \mathbf{x}_j to its k -th nearest neighbor $\mathbf{x}_j^{(k)}$. It is interesting to evaluate the sensitivity of inv-DAKR and bi-DAKR to parameter k . To this end, we compute the average performance gains of inv-DAKR and bi-DAKR over the baseline algorithm (k -NN) for accuracy at rank-1 and rank-5, and show each of them as a function of the local parameter k in Fig. 2. The average is taken over all 38 sets of experimental results, where the shadow indicates the standard deviation. As can be observed: a) Our proposed inv-DAKR and bi-DAKR are not too sensitive to the parameter k when k is not too small; b) Compared to inv-DAKR, bi-DAKR is more promising when $k > 3$. By default, it is a good practice to set $k = 30$.

TABLE III
COMPARISON ON GRID, PRID450S, VIPeR, AND CUHK03 WITH DIFFERENT FEATURES.

Feature	Methods	GRID			PRID450S			VIPeR			CUHK03(labeled)			CUHK03(detected)		
		r=1	r=10	r=20	r=1	r=10	r=20	r=1	r=10	r=20	r=1	r=5	r=10	r=1	r=5	r=10
LOMO	k -NN	16.56	41.84	52.40	59.78	90.09	95.29	41.08	82.34	91.27	50.85	81.38	91.14	44.45	78.70	87.65
	k -INN	21.52	44.88	55.68	51.38	90.04	94.58	35.32	82.25	90.85	40.14	80.73	90.74	36.65	78.15	88.75
	k -RNN	19.44	42.96	54.56	45.51	84.80	91.69	29.40	77.47	90.28	40.74	78.03	89.09	36.70	73.35	84.65
	inv-DAKR	19.84	45.44	56.24	59.24	90.44	95.29	41.61	83.10	91.84	52.56	83.08	91.74	47.35	79.90	89.75
	bi-DAKR	19.60	44.48	56.40	61.42	92.40	96.93	42.97	83.86	92.41	53.45	84.74	92.84	48.10	80.80	90.05
	bi-DAKR [†]	19.60	44.48	56.40	61.42	92.44	96.93	42.94	83.86	92.44	53.50	84.74	92.89	48.10	80.80	90.05
	bi-DAKR [‡]	19.68	44.40	56.40	61.56	92.40	96.93	43.01	83.89	92.41	53.45	84.43	92.69	47.90	80.60	90.10
GOG	k -NN	24.80	58.40	68.88	68.00	94.36	97.64	49.68	88.67	94.53	68.47	90.69	95.84	64.10	88.40	94.30
	k -INN	27.44	57.84	68.56	53.11	94.22	97.60	41.61	87.41	94.59	52.50	90.49	96.95	49.10	87.55	94.35
	k -RNN	24.40	56.40	67.20	47.38	90.22	96.09	34.18	83.16	92.88	56.26	87.28	94.54	52.20	85.80	92.30
	inv-DAKR	26.00	58.00	68.72	65.02	94.98	98.00	48.73	89.18	94.97	70.32	92.54	97.20	67.20	90.30	95.60
	bi-DAKR	27.12	60.16	70.96	68.98	95.82	98.62	50.66	90.19	95.51	71.87	93.24	97.70	68.80	90.50	95.80
	bi-DAKR [†]	27.12	60.16	70.96	68.98	95.87	98.62	50.63	90.22	95.51	71.87	93.24	97.70	68.80	90.50	95.80
	bi-DAKR [‡]	27.12	60.00	70.88	69.02	95.82	98.58	50.60	90.16	95.47	71.82	93.29	97.80	68.80	90.55	95.60
Fusion	k -NN	27.04	59.36	70.00	72.04	95.96	98.53	53.26	90.95	95.73	71.87	92.64	96.80	68.05	90.15	94.95
	k -INN	28.00	58.96	68.56	55.38	95.33	97.96	43.80	89.78	95.25	53.55	91.99	97.50	50.30	89.65	95.60
	k -RNN	25.60	57.12	67.60	49.07	91.38	96.44	37.44	85.73	93.73	59.81	90.34	95.64	56.10	87.25	93.35
	inv-DAKR	28.16	59.60	69.84	68.58	96.00	98.44	52.53	90.57	95.89	73.53	94.24	98.15	70.65	92.10	96.25
	bi-DAKR	28.00	61.52	71.36	73.16	97.02	99.11	54.34	91.58	96.33	75.08	95.14	98.35	72.85	92.05	96.45
	bi-DAKR [†]	28.00	61.52	71.36	73.16	97.02	99.11	54.30	91.58	96.33	75.03	95.14	98.35	72.85	92.00	96.45
	bi-DAKR [‡]	28.08	61.52	71.28	73.11	96.98	99.11	54.30	91.58	96.30	74.93	95.09	98.35	72.85	92.15	96.55
	re-ranking[24]	28.00	60.40	70.64	72.36	96.27	98.71	53.70	91.65	96.65	73.42	93.74	97.29	69.60	91.50	95.55
	SSM[25]	27.20	61.12	70.56	72.98	96.76	99.11	53.73	91.49	96.08	76.63	94.59	97.95	72.70	92.40	96.05

TABLE IV
COMPARISON ON MARKET-1501 WITH RESNET-50-IDE FEATURES IN DIFFERENT METRICS.

Feature	Methods	r=1	r=5	r=10	mAP
Euc	k -NN	75.62	87.95	91.89	50.68
	inv-DAKR	76.40	88.48	92.46	51.81
	bi-DAKR	76.57	88.93	92.84	51.88
	re-ranking[24]	78.27	86.67	90.02	65.80
	XQDA	k -NN	75.39	88.60	91.69
inv-DAKR		77.26	89.28	92.79	54.62
bi-DAKR		76.90	89.43	93.23	54.78
re-ranking[24]		77.91	85.90	89.76	66.71
KISSME		k -NN	77.52	89.46	93.02
	inv-DAKR	79.28	90.35	93.68	55.63
	bi-DAKR	78.95	90.64	94.03	55.70
	re-ranking[24]	81.56	87.53	90.38	70.10
	Mahal	k -NN	77.20	89.82	92.99
inv-DAKR		78.95	90.17	93.65	55.07
bi-DAKR		78.56	90.86	93.97	55.04
re-ranking[24]		81.12	88.03	90.91	69.82

TABLE V
COMPARISON ON MARS WITH IDE FEATURES AND IN DIFFERENT METRICS.

Metric	Methods	r=1	r=5	r=20	mAP
Euc	k -NN	65.51	81.72	90.10	46.67
	inv-DAKR	66.77	82.68	91.21	48.53
	bi-DAKR	66.57	82.88	91.46	48.43
	re-ranking[24]	67.68	82.17	90.91	58.25
	XQDA	k -NN	64.95	81.01	89.90
inv-DAKR		65.15	82.58	90.56	47.72
bi-DAKR		66.36	82.63	91.67	47.72
re-ranking[24]		67.17	81.41	90.25	57.33
KISSME		k -NN	63.33	80.51	88.74
	inv-DAKR	63.89	80.81	89.65	45.63
	bi-DAKR	65.15	81.67	91.01	46.11
	re-ranking[24]	65.71	80.51	89.29	55.53
	Mahal	k -NN	60.81	77.93	87.88
inv-DAKR		61.92	78.38	88.28	42.77
bi-DAKR		61.81	79.14	88.69	42.90
re-ranking[24]		63.59	78.43	88.18	51.93

TABLE VI
COMPARISON ON COMPUTATION TIME COSTS.

Datasets	Size	Methods	Time
CHUK03	200	inv-DAKR	0.0900s
		bi-DAKR	0.0876s
		re-ranking[24]	0.3060s
PRID450s	450	inv-DAKR	0.1368s
		bi-DAKR	0.1301s
		re-ranking[24]	0.6065s
VIPeR	632	inv-DAKR	0.2695s
		bi-DAKR	0.2571s
		re-ranking[24]	0.9894s
GRID	1025	inv-DAKR	0.7749s
		bi-DAKR	0.7772s
		re-ranking[24]	2.3126s
Mars	12180	inv-DAKR	3.3053s
		bi-DAKR	4.0052s
		re-ranking[24]	30.3338s
Market-1501	19732	inv-DAKR	7.1679s
		bi-DAKR	8.0736s
		re-ranking[24]	80.6114s

V. CONCLUSION

We investigated the density-adaptive kernel techniques for efficient and effective re-ranking in person ReID. Specifically, we presented two Density-Adaptive Kernel based Re-ranking (DAKR) approaches: inverse DAKR and bidirectional DAKR, in which a smooth kernel function equipped with a density-adaptive parameter is exploited to not only accommodate the ambiguity and local density information in finding matched results but also reduce the computational cost. Experiments on six benchmark data sets have validated the efficiency and effectiveness of our proposals.

ACKNOWLEDGMENT

R. Guo, J. Lin, and Y. Li are supported by the National Natural Science Foundation of China under Grant No. 61771066. C.-G. Li is supported partially by the Open Project Fund from

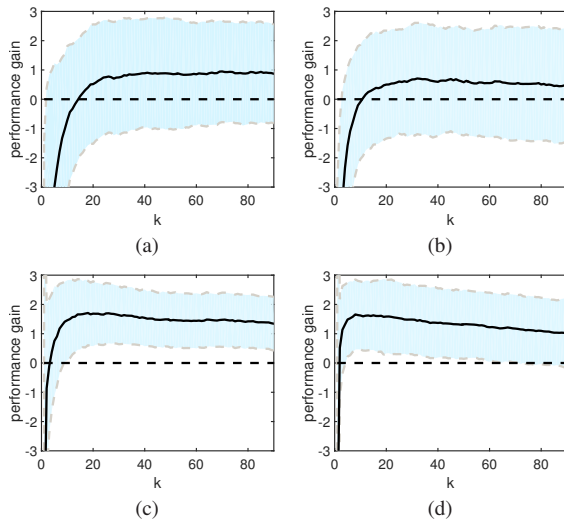


Fig. 2. Average performance gain as a function of k . (a): inv-DAKR (rank-1). (b): inv-DAKR (rank-5). (c): bi-DAKR (rank-1). (d): bi-DAKR (rank-5).

the Key Laboratory of Machine Perception (MOE), Peking University.

REFERENCES

- [1] S. Gong, M. Cristani, S. Yan, and C. C. Loy, *Person Re-identification*. Springer, 2014.
- [2] N. Dalal and B. Triggs, "Histograms of oriented gradients for human detection," in *IEEE Conference on Computer Vision and Pattern Recognition*, 2005, pp. 886–893.
- [3] N. Dalal, B. Triggs, and C. Schmid, "Human detection using oriented histograms of flow and appearance," in *European Conference on Computer Vision*, 2006, pp. 428–441.
- [4] C. Liu, S. Gong, C. C. Loy, and X. Lin, "Person re-identification: what features are important?" in *European Conference on Computer Vision*, 2012, pp. 391–401.
- [5] Y. Yang, J. Yang, J. Yan, S. Liao, D. Yi, and S. Z. Li, "Salient color names for person re-identification," in *European Conference on Computer Vision*, vol. 8689, 2014, pp. 536–551.
- [6] J. Si, H. Zhang, C.-G. Li, and J. Guo, "Spatial pyramid-based statistical features for person re-identification: A comprehensive evaluation," *IEEE Transactions on Systems, Man, and Cybernetics: Systems*, 2017.
- [7] S. C. Dong, M. Cristani, M. Stoppa, L. Bazzani, and V. Murino, "Custom pictorial structures for re-identification," in *British Machine Vision Conference*, 2011, pp. 68.1–68.11.
- [8] N. Gheissari, T. B. Sebastian, and R. Hartley, "Person reidentification using spatiotemporal appearance," in *IEEE Conference on Computer Vision and Pattern Recognition*, 2006, pp. 1528–1535.
- [9] Y. Hu, S. Liao, Z. Lei, D. Yi, and S. Z. Li, "Exploring structural information and fusing multiple features for person re-identification," in *IEEE Conference on Computer Vision and Pattern Recognition*, 2013, pp. 794–799.
- [10] D. Gray and H. Tao, "Viewpoint invariant pedestrian recognition with an ensemble of localized features," in *European Conference on Computer Vision*, 2008, pp. 262–275.
- [11] X. Wang, G. Doretto, T. Sebastian, P. Tu, and J. Rittscher, "Shape and appearance context modeling," in *IEEE International Conference on Computer Vision*. Rio de Janeiro, 2007, pp. 1–8.
- [12] T. Matsukawa, T. Okabe, E. Suzuki, and Y. Sato, "Hierarchical gaussian descriptor for person re-identification," in *IEEE Conference on Computer Vision and Pattern Recognition*, 2016, pp. 1363–1372.
- [13] S. Liao, Y. Hu, X. Zhu, and S. Z. Li, "Person re-identification by local maximal occurrence representation and metric learning," in *IEEE Conference on Computer Vision and Pattern Recognition*, 2015, pp. 2197–2206.
- [14] J. Si, H. Zhang, C.-G. Li, J. Kuen, X. Kong, A. Kot, and G. Wang, "Dual attention matching networks for context-aware feature sequence based person re-identification," in *CVPR*, 2018.
- [15] J. V. Davis, B. Kulis, P. Jain, S. Sra, and I. S. Dhillon, "Information-theoretic metric learning," in *International Conference on Machine Learning*, 2007, pp. 209–216.
- [16] M. Dikmen, E. Akbas, T. S. Huang, and N. Ahuja, "Pedestrian recognition with a learned metric," in *Asian Conference on Computer Vision*, 2010, pp. 501–512.
- [17] M. Kostinger, M. Hirzer, P. Wohlhart, P. M. Roth, and H. Bischof, "Large scale metric learning from equivalence constraints," in *IEEE Conference on Computer Vision and Pattern Recognition*, 2012, pp. 2288–2295.
- [18] Z. Li, S. Y. Chang, F. Liang, T. S. Huang, L. L. Cao, and J. R. Smith, "Learning locally-adaptive decision functions for person verification," in *IEEE Conference on Computer Vision and Pattern Recognition*, 2013, pp. 3610–3617.
- [19] K. Q. Weinberger, J. Blitzer, and L. K. Saul, "Distance metric learning for large margin nearest neighbor classification," in *Conference on Neural Information Processing Systems*, 2006, pp. 1473–1480.
- [20] W. S. Zheng, S. Gong, and T. Xiang, "Person re-identification by probabilistic relative distance comparison," in *IEEE Conference on Computer Vision and Pattern Recognition*, 2011, pp. 649–656.
- [21] J. Si, H. Zhang, and C.-G. Li, "Regularization in metric learning for person re-identification," in *ICIP*, 2015, pp. 2309–2313.
- [22] C. Liu, C. L. Chen, S. Gong, and G. Wang, "POP: Person re-identification post-rank optimisation," in *IEEE International Conference on Computer Vision*, 2013, pp. 441–448.
- [23] H. Wang, S. Gong, X. Zhu, and T. Xiang, "Human-in-the-loop person re-identification," in *European Conference on Computer Vision*, 2016, pp. 405–422.
- [24] Z. Zhong, L. Zheng, D. Cao, and S. Li, "Re-ranking person re-identification with k-reciprocal encoding," in *IEEE Conference on Computer Vision and Pattern Recognition*, 2017, pp. 3652–3661.
- [25] S. Bai, X. Bai, and Q. Tian, "Scalable person re-identification on supervised smoothed manifold," in *IEEE Conference on Computer Vision and Pattern Recognition*, 2017, pp. 3356–3365.
- [26] R. Yu, Z. Zhou, S. Bai, and X. Bai, "Divide and fuse: A re-ranking approach for person re-identification," in *British Machine Vision Conference*, 2017.
- [27] D. Qin, S. Gammeter, L. Bossard, T. Quack, and L. van Gool, "Hello neighbor: Accurate object retrieval with k-reciprocal nearest neighbors," in *IEEE Conference on Computer Vision and Pattern Recognition*, 2011, pp. 777–784.
- [28] Q. Leng, R. Hu, C. Liang, Y. Wang, and J. Chen, "Person re-identification with content and context re-ranking," *Multimedia Tools Appl.*, vol. 74, no. 17, pp. 6989–7014, 2015.
- [29] S. Bai and X. Bai, "Sparse contextual activation for efficient visual re-ranking," *IEEE Transactions on Image Processing*, vol. 25, no. 3, pp. 1056–1069, 2016.
- [30] Q. Leng, R. Hu, C. Liang, Y. Wang, and J. Chen, "Bidirectional ranking for person re-identification," in *IEEE International Conference on Multimedia and Expo*, 2013, pp. 1–6.
- [31] J. Garcia, N. Martinel, A. Gardel, I. Bravo, G. L. Foresti, and C. Micheloni, "Discriminant context information analysis for post-ranking person re-identification," *IEEE Transactions on Image Processing*, vol. 26, no. 4, pp. 1650–1665, 2017.
- [32] F. Korn and S. Muthukrishnan, "Influence sets based on reverse nearest neighbor queries," *Acm Sigmod Record*, vol. 29, pp. 201–212, 2000.
- [33] L. Zelnik-manor and P. Perona, "Self-tuning spectral clustering," *Advances in Neural Information Processing Systems*, vol. 17, pp. 1601–1608, 2004.
- [34] C. L. Chen, T. Xiang, and S. Gong, "Time-delayed correlation analysis for multi-camera activity understanding," *International Journal of Computer Vision*, vol. 90, no. 1, pp. 106–129, 2010.
- [35] P. M. Roth, M. Hirzer, M. Köstinger, C. Belezni, and H. Bischof, "Mahalanobis distance learning for person re-identification," in *IEEE Conference on Computer Vision and Pattern Recognition*, 2014, pp. 247–267.
- [36] W. Li, R. Zhao, T. Xiao, and X. Wang, "DeepReID: Deep filter pairing neural network for person re-identification," in *IEEE Conference on Computer Vision and Pattern Recognition*, 2014, pp. 152–159.
- [37] L. Zheng, L. Shen, L. Tian, S. Wang, J. Wang, and Q. Tian, "Scalable person re-identification: A benchmark," in *IEEE International Conference on Computer Vision*, 2015, pp. 1116–1124.

- [38] L. Zheng, Z. Bie, Y. Sun, J. Wang, C. Su, S. Wang, and Q. Tian, "MARS: A video benchmark for large-scale person re-identification," in *European Conference on Computer Vision*, 2016, pp. 868–884.